

Prospects toward flexible magnonic systems

Cite as: J. Appl. Phys. **130**, 150901 (2021); <https://doi.org/10.1063/5.0055976>

Submitted: 05 May 2021 • Accepted: 04 October 2021 • Published Online: 18 October 2021

 D. Faurie,  A. O. Adeyeye and  F. Zighem



View Online



Export Citation



CrossMark

ARTICLES YOU MAY BE INTERESTED IN

Skyrmion based magnonic crystals

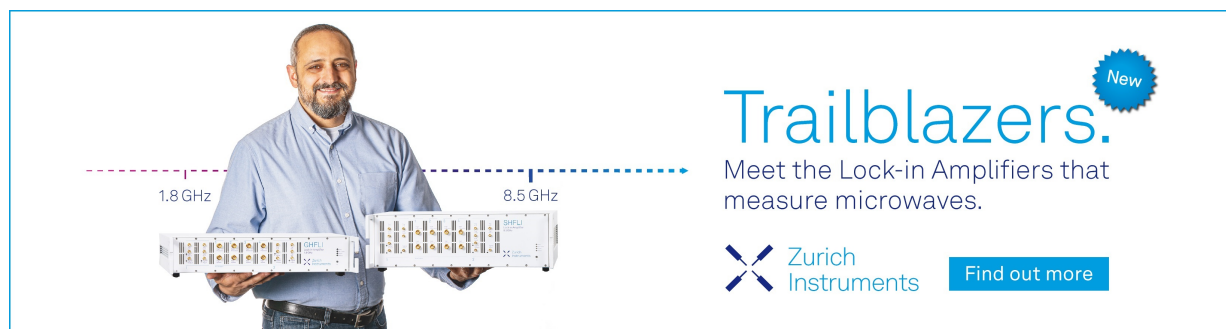
Journal of Applied Physics **130**, 090901 (2021); <https://doi.org/10.1063/5.0061832>


Widefield quantum microscopy with nitrogen-vacancy centers in diamond: Strengths, limitations, and prospects

Journal of Applied Physics **130**, 150902 (2021); <https://doi.org/10.1063/5.0066733>


Mesoscopic magnetic systems: From fundamental properties to devices

Applied Physics Letters **119**, 080401 (2021); <https://doi.org/10.1063/5.0064083>



Trailblazers. 

Meet the Lock-in Amplifiers that measure microwaves.

 Zurich Instruments [Find out more](#)

Prospects toward flexible magnonic systems

Cite as: J. Appl. Phys. **130**, 150901 (2021); doi: [10.1063/5.0055976](https://doi.org/10.1063/5.0055976)

Submitted: 5 May 2021 · Accepted: 4 October 2021 ·

Published Online: 18 October 2021



D. Faurie,^{1,a)} A. O. Adeyeye,^{2,3} and F. Zighed^{1,b)}

AFFILIATIONS

¹LSPM-CNRS, UPR3407, Université Sorbonne Paris Nord, 93430 Villetaneuse, France

²Information Storage Materials Laboratory, Department of Electrical and Computer Engineering, National University of Singapore, 117576 Singapore, Singapore

³Department of Physics, Durham University, South Road, Durham DH1 3LE, United Kingdom

^{a)}Author to whom correspondence should be addressed: faurie@univ-paris13.fr

^{b)}Electronic address: zighed@univ-paris13.fr

ABSTRACT

This paper presents the prospects for periodic magnetic nanostructures in the form of magnonic crystals on polymer substrates. Indeed, arrays of magnetic nanostructures on flexible substrates are promising for microwave applications in the GHz frequency range. In particular, the mastery of the potentially coupled physical properties (magnetic and mechanical) allows one to consider devices for microelectronics in general, combining the microwave properties of spin waves with the lightness and conformability of polymer substrates. However, there are still scientific hurdles to be overcome, particularly with regard to the reliability of these systems, which is the focus of this review. Subsequently, we propose a general state of the art, a summary of the precursor works, and a general strategy for the optimization of these systems and their future possibilities.

Published under an exclusive license by AIP Publishing. <https://doi.org/10.1063/5.0055976>

I. INTRODUCTION

Devices fabricated on flexible substrates have been extensively studied because of their outstanding potential for new applications requiring non-planar functional systems.^{1,2} Indeed, most objects of everyday life as well as objects with industrial or military applications are not flat and rigid but curved and deformable, such as sheets of paper and textiles. The fields of application are numerous, ranging from everyday electronic gadgets to the most advanced telecommunication systems. During the last ten years, several electronic devices (flexible solar cells, light-emitting diodes, transistors, etc.) have been realized on top of various polymeric substrates.^{3–16} Particularly, systems based on magnetic thin films on polymer substrates have recently shown a very strong interest in the fields of flexible or scalable magnetoelectronics^{17–22} (see Fig. 1). The integration of magnetic functions on flexible/stretchable substrates can have many advantages for many users²³ but also create new applications, such as flexible displays or magnetoelectric sensors.²⁴ Moreover, it is known that polymer substrates are light and inexpensive.

It is important to imagine modern flexible systems with great potential for the future. Therefore, technologies already developed

on rigid substrates should be explored and applied to polymeric substrates. Concerning data storage or sensors, the most developed applications on flexible substrates are mainly systems using the giant magnetoresistance (GMR) property.²⁰ The spin Hall effect²⁵ and the magneto-impedance property²⁶ have also been used to develop new flexible magnetic systems. However, all these technologies will reach the same miniaturization limits for data storage and transfer as those encountered for “classical” substrates. The developments are still in their infancy, and the possibilities of lateral nanostructuring, in particular, allow us to foresee further potentialities for these flexible magnetic systems.²⁷ Indeed, the realization of functional, flexible, and stretchable magnetic micro- and nanostructures may lead to a new generation of magnetic materials for sensing and recording as well as magneto-optical and magneto-phonic devices.²³ The current generation of those technologies, utilizing more traditional substrate technologies, has been highly successful. This suggests that the new generation with added functionalities will also be a success.

Among the solutions that have not yet been tested on polymer substrates, magnonic systems taking advantage of spin-wave properties for data transfer are potentially very interesting.^{28,29} Indeed, the flexibility of polymers offers solutions for the incorporation of

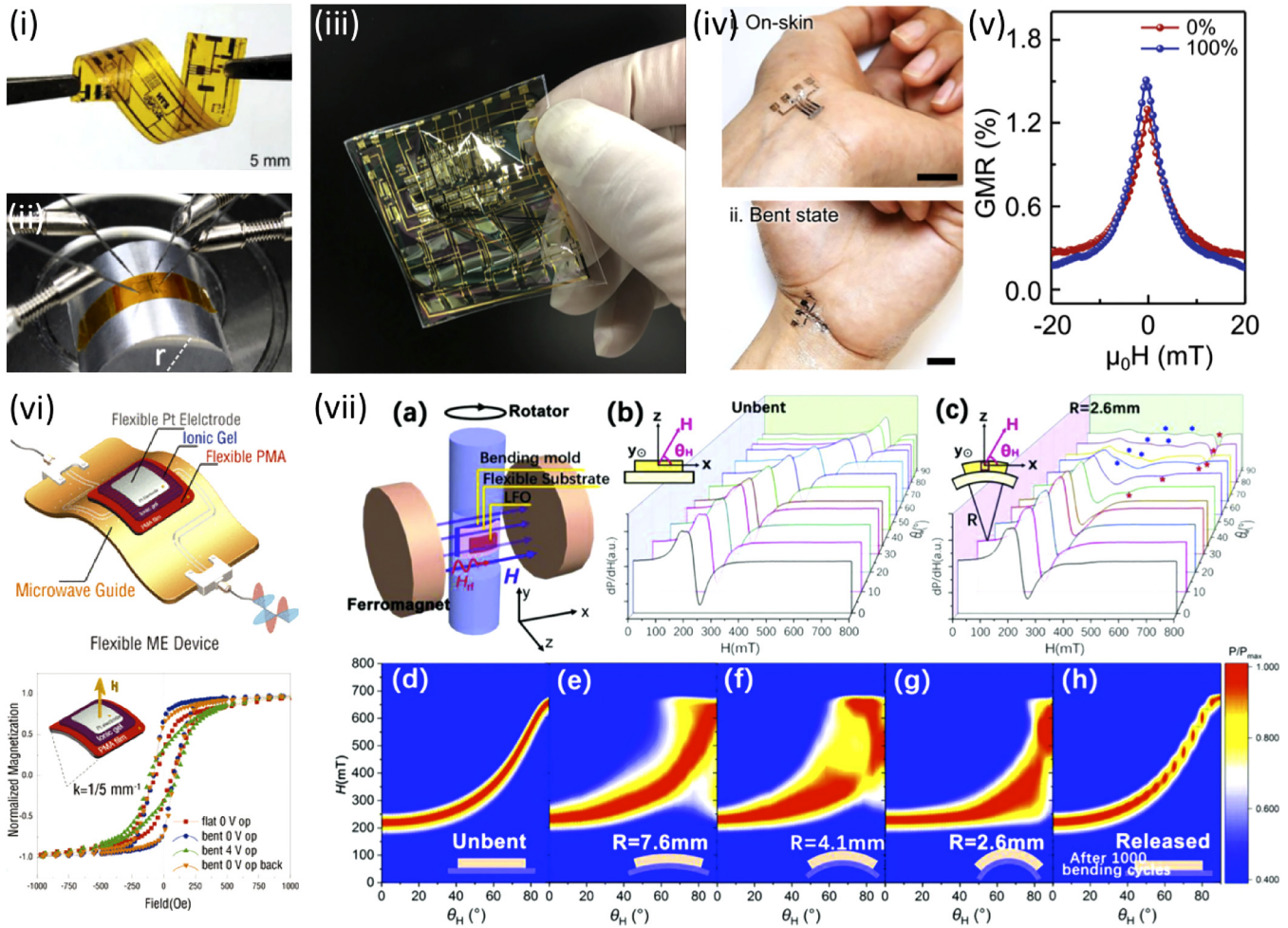


FIG. 1. (i) Magnetosensitive e-skins conditioned with inorganic electronics on-foil. Examples of entirely flexible magnetosensitive e-skins as pliable devices.¹⁷ (ii) Image of a magnetoresistance measurement setup of a TMR on Kapton® under bending. Reproduced with permission from Bedoya-Pinto *et al.*, Appl. Phys. Lett. **104**, 062412 (2014). Copyright 2014 AIP Publishing LLC.¹⁸ (iii) Active magnetosensory matrix circuit fabricated on a single parylene wafer.¹⁹ (iv) Photographs of printed GMR sensors conformably applied on skin with curved body parts of a stretched (i) and bent (ii) wrist.²⁰ (v) GMR performance of a printed sensor in the relaxed (0 stretching) and stretched state (100% stretching).²⁰ (vi) Concept demonstration of a low-voltage tunable RF/microwave device based on flexible laminates. Magnetization curve evolution during an *in situ* ionic gel gating process along the in-plane direction of a bent film. Adapted with permission from Zhao *et al.*, ACS Nano **12**, 7167 (2018). Copyright 2018 American Chemical Society.²¹ (vii) (a) Schematic illustration of an FMR spectroscopy experimental setup for a sample under bending. Out-of-plane angular dependent FMR spectra for a T-LFO (001) film with (b) unbent and (c) bending status. (d)–(h) Counterplot of the out-of-plane angular dependent-integrated FMR spectra for the T-LFO (001) film with different bending states.²²

magnonic systems in confined and geometrically complex spaces. For this purpose, conventional rigid substrates must be replaced by compliant substrates such as polymers. Magnonic crystals are arrays of magnetic nanostructures with periodic lateral variations of their magnetic properties, which are magnetic analogs of photonic and phononic crystals.^{30–33} Indeed, the propagation of spin waves in periodically structured materials is of profound interest to the physics research community and industry. Naturally, magnetic nanostructures represent non-volatile memory elements; therefore, their deposition on polymeric substrates would allow flexible/

stretchable programmable devices with ultrafast reprogramming on sub-nanosecond time scales.^{34–36} Furthermore, for applications in magnetic data storage media, magnetic nanostructures can be combined with nanoelectronics (e.g., in read heads and magnetic random access memories³⁷) and optics (e.g., in magneto-optical disks³⁸). From a practical point of view, the most attractive feature of magnonic crystals is that they can easily change the dispersion spectrum of spin waves through an external magnetic field (Fig. 2).

Despite their potentialities, flexible magnonic systems have not yet been fully realized in the nanomagnetism community.

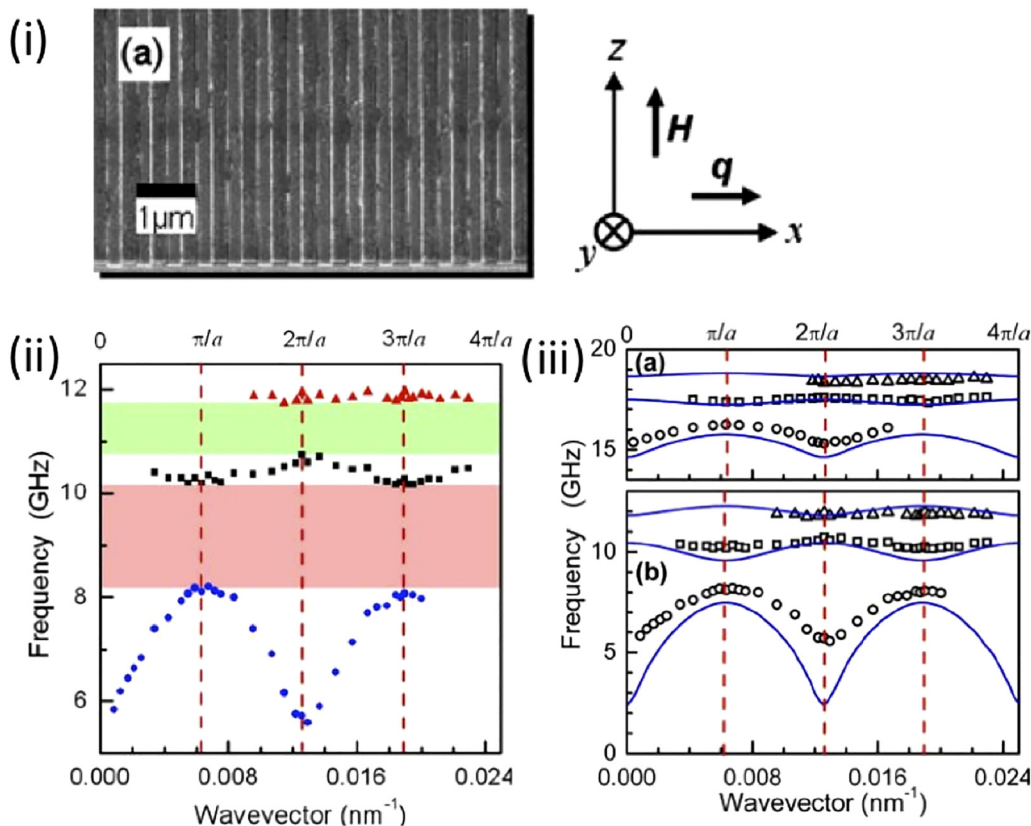


FIG. 2. (i) Image of a 1D bicomponent (Co and $\text{Ni}_{80}\text{Fe}_{20}$) magnonic crystal (periodicity of $a = 500$ nm). (ii) Magnonic band structures of this crystal measured by Brillouin light scattering highlighting two magnonic bandgaps in an extended representation ($\frac{\pi}{a}, \frac{2\pi}{a}, \dots$ to the first, second, \dots Brillouin zone). (iii) Experimental and simulated band structures (a) in the absence and (b) the presence ($H = 2$ kOe) of an applied magnetic field showing the strong dependence of the band position and width with an applied magnetic field. Reproduced with permission from Wang *et al.*, Appl. Phys. Lett. **94**, 083112 (2009). Copyright 2009 AIP Publishing LLC.

Contrary to the already conventional notions of “flexible photonics,”^{39,40} “flexible plasmonics,”^{41,42} or more generally “flexible electronics,” the term “flexible magnonics” has not been introduced into the literature yet. This is really surprising because the spin-wave technology holds great potential as a new platform for information processing and data storage devices,²⁹ including flexible ones. Responses of conventional magnonic devices (on rigid substrates) can be easily controlled by an applied magnetic field. On the other side, flexible magnonic crystals are intended to be used in devices that will be exposed to repeated large strains during use. Therefore, their responses will be affected by elastic strains (magnetoelastic effect) in addition to irreversible effects such as damaging (cracks). However, the investigation of spin-wave propagation in patterned thin films on polymer substrates has not been carried out so far.

These flexible magnonic crystals could open a new era in light and flexible electronics with many advantages. First, spin waves can be easily generated and manipulated in magnetic systems.³¹ They can be thermally activated at room temperature and can be manipulated by a magnetic field. Second, like light in optical fibers, spin waves can

be directed in magnetic guides made of ferromagnetic materials, which are attenuated depending on the magnetic damping and other magnetic parameters (anisotropy, exchange, \dots). The propagation distance is generally of a few microns for nanometric thin film alloys (permalloy, CoFeB, YIG, \dots).²⁹ Finally, and this is their main advantage, spin waves can have a very short wavelength and a high “coherence length” (several hundred microns), which means that the properties of the waves are preserved over distances much larger than the size of nanoscale devices.^{43–46} The spatial and temporal scales associated with spin waves (nanometer and picosecond) are precisely those that suggest the possibility of designing extremely small electronic devices dedicated to signal processing that would combine the advantages of magnetic devices (non-volatility) and waves. To be applied in flexible microelectronics, these systems must be integrated in the presence of microwave circuits. The latter must be specific with a very good mechanical resistance. This can be achieved with few materials whose ductility is sufficient to be subjected to repeated deformations. Common materials are, for example, gold and copper for metals. Indeed, these materials can withstand large cyclic deformations (over 10%).⁴⁷

In this Perspective, we will first introduce a short state of the art of the last few years on magnonic crystals as well as pioneering work on flexible magnetic systems. Then, we will address the first works dealing with the effects of strains on magnetic modes (especially localized) in nanostructured systems on flexible substrates. We will also mention the pioneering work on the modeling of the static and dynamic magnetization in nanostructures deformed by a substrate. Finally, we will discuss the strategies to be adopted in order to develop the field of flexible magnonics and the different fundamental and applicative perspectives that can be envisaged.

II. STATE OF THE ART

A. Magnonic crystals

Recently, there has been growing interest in the fundamental understanding of spin-wave propagation in magnonic crystals because of their huge potential in a wide range of applications such as microwave resonators,²⁹ filters,⁴⁸ and spin-wave logic devices.⁴⁹ From a practical viewpoint, the most attractive features of magnonic crystals are that the dispersion spectrum of magnons can be easily modified by an external magnetic field.

The use of periodic magnetic nanostructures as a functional medium in magnonic devices offers advantage over conventional charge based devices since both the amplitude and direction (phase) of magnetization can be used for information encoding when compared to a scalar charge.³⁵ The encoding of information into the magnetization amplitude immediately leads to a spin-wave switch—a device that can transmit or stop the propagation of spin waves. If information is encoded in phase, different frequencies can be used as separate information channels allowing for parallel data processing in the same structure.⁵⁰ The ability to transmit and process information in a multichannel manner provides a fundamental advantage over existing switch based logic devices. Importantly, the shape anisotropy in nano-confined geometries may play the role of the biasing external field, and devices may operate at gigahertz frequencies with just a small external biasing or without it at all. Spectra of spin-wave excitations in magnonic crystals are significantly different from those of uniform media. Due to the lateral periodic magnetic contrasts, they exhibit features such as tunable magnonic bandgaps, where spin-wave propagation is entirely prohibited. The existence of spin-wave bandgaps has been predicted for one-dimensional,³¹ two-dimensional,³⁰ and three-dimensional systems.⁵² Frequency bandgaps have been observed experimentally in wire-like structures consisting of shallow grooves etched into yttrium-iron-garnet films, a one-dimensional array of homogenous $\text{Ni}_{80}\text{Fe}_{20}$ nanowires separated by an air gap,^{53,54} and synthetic nanostructures composed of periodic arrays of alternating $\text{Ni}_{80}\text{Fe}_{20}$ nanowires in direct contact with Co nanowires, also known as “bi-component magnonic crystals.”⁵⁵ It has been clearly shown that the frequency bandgaps can be tuned by the application of a magnetic field and also by changing the lateral dimensions of the nanowires.³³ Moreover, this bandgap structure could be tuned also by a strain-induced magnetic field (due to the magnetoelastic energy). This bandgap tunability is an important property, which could find applications in the control of the generation and propagation of information-carrying spin waves

in devices based on these crystals.^{56–58} By adjusting the size of the bandgap (where spin wave propagation is completely forbidden), only modes capable of crossing the gap could propagate through the medium, with selective propagation of certain spin-wave frequencies. Moreover, the recent development of artificial spin-ice opens up unexplored fields for the exploitation of spin wave properties.^{59,60} Therefore, the development of systems using magnons is a promising approach to information processing in the coming decades.⁵¹ Magnonic crystals on polymer substrates thus allow one to consider various applications such as a strain controllable multi-channel telecommunication system. To achieve these objectives, however, there are specificities of flexible systems to be understood, in particular, their mechanical properties and the coupling between strain fields and magnetic properties.

B. Flexible systems

Integration of magnetic features into the flexible objects may provide numerous users with a number of benefits and also give rise to new applications such as flexible displays or magnetoelectric sensors.^{61–65} The time is now ripe for designing flexible systems with high potential for the future. Hence, it is advantageous to use them as substrates for magnetic nanostructures; this requires adaptation of the existing expertise, technologies, and techniques to the polymer substrates. Until now, much work on polymer substrates has been carried out on continuous thin film systems but very little in the form of periodic nanostructures. At the level of fundamental studies, the work of the 2000s consisted of studying the relations between macroscopic strain and magnetic properties of ferromagnetic films. The main experimental developments have focused on the development of *in situ* experiments such as magneto-optical Kerr effect magnetometry (MOKE) or FMR combined with bending or tensile tests. In addition to simple magnetic films, the systems studied were mostly magneto-resistive [Giant Magnetoresistance (GMR) or Tunnel Magnetoresistance (TMR)] systems.^{66–68}

Since 2010, the study of these properties under very high strains, simple or cyclic, has shown that it is possible to develop deformable and reliable magnetoresistive sensors that can adapt to the most complex geometries (surfaces with strong curvatures)^{69,70} despite the fact that many damages can occur in the nanometric layers.^{71,72} Indeed, even if multiple cracks or local decohesions only slightly alter the magnetoresistance properties, these effects are not negligible and could have stronger repercussions on the magnetic properties of systems based on spin waves, for example. Indeed, Merabine *et al.* have recently shown that thin film damage induces important mechanical stresses and significantly modify the anisotropy field and the magnetic damping.⁷² This is all the more the case as the magnetoelastic coefficients of thin films are high.

It is important to find solutions to avoid or at least delay these damages in magnetic systems. There are existing methods such as depositing thin films on an elastomer substrate under tension and then relaxing the system.^{71,73,74} This has the effect of creating wrinkles that then delay damage when stretched again. Otherwise, it so happens that nanostructuring seems to be a relevant way to get around this problem as we will see in Sec. III. Indeed, for reasons of strain distributions between flexible substrates and

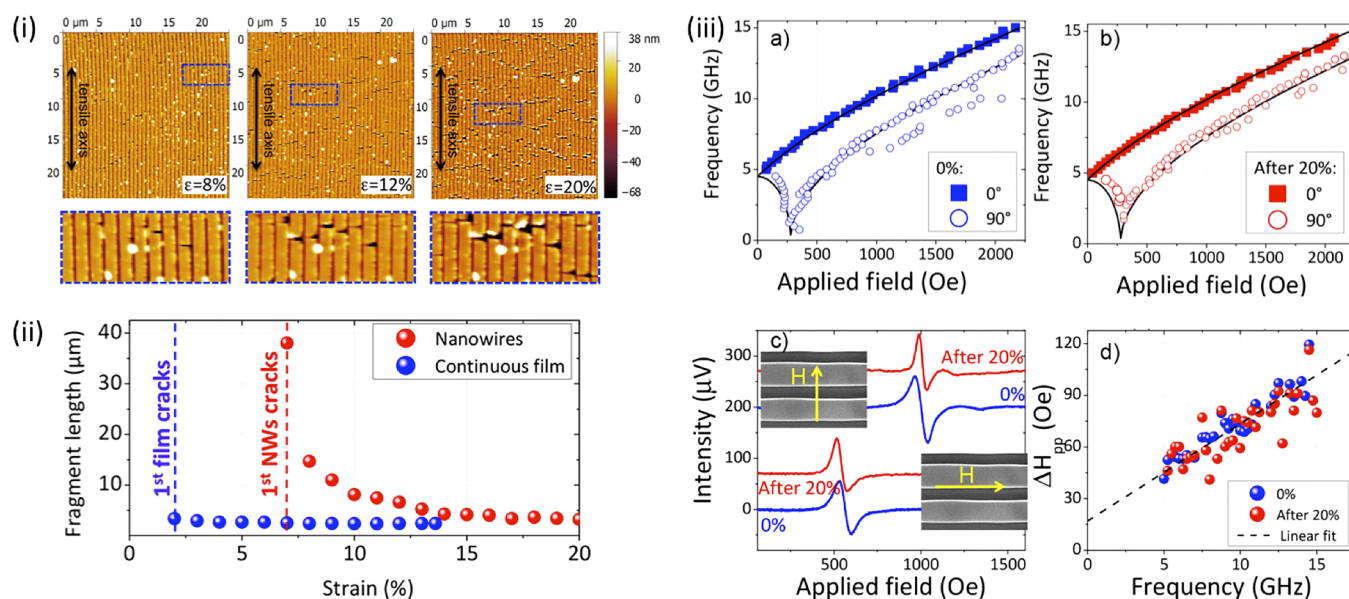


FIG. 3. (i) Typical AFM images highlighting the multicracking of a 20 nm thick $\text{Ni}_{80}\text{Fe}_{20}$ array of nanowires on a Kapton substrate at different strain states (8%, 12%, and 20%). (ii) Residual fragment length as a function of the applied strains of $\text{Ni}_{80}\text{Fe}_{20}$ film and arrays of nanowires (NWs). (iii) (a) and (b) Frequency dependencies as a function of applied magnetic field along and perpendicular to the nanowires for a $\text{Ni}_{80}\text{Fe}_{20}$ array of nanowires. The dependencies are presented for two stresses states: at 0% (a) and at 20% (b). (c) Typical FMR spectra of the NWs for a magnetic field applied along and perpendicular to the NWs at 0% of strain and after 20% of strain. (d) Peak to peak FMR linewidth ΔH_{pp} variations as a function of the frequency obtained from the spectra recorded with a magnetic field applied along the NWs. The dashed line is a linear fit and serves as a guide for the eyes. Adapted with permission from Merabtine *et al.*, *Nano Lett.* **18**, 3199 (2018). Copyright 2018 American Chemical Society.⁷⁵

nanostructures, it is quite possible to delay the appearance of cracks.⁷⁵ Merabtine *et al.* showed that lateral nanostructuring could be a way to delay damage (cracks); see Fig. 3. Indeed, for a given material thickness, he showed that the initiation of multicracking of nanowires was much later than that of a continuous film ($\epsilon = 7\%$ instead of 2%). This is shown in Figs. 3(i) and 3(ii) for $\text{Ni}_{80}\text{Fe}_{20}$ systems. For this same system, Merabtine *et al.* also showed that the magnetic anisotropy was insensitive to the multiplication of cracks, at least up to 20% of strain [Fig. 3(iii) (a) and (b)]. This is because the average fragment length at saturation of the multicracking (about 3 μm) is sufficient to retain the initial shape anisotropy. It is also interesting to see that the FMR linewidths are also very insensitive to these damages, as shown in Fig. 3(iii) (c) and (d), linked, in particular, to the weak magnetostriction of $\text{Ni}_{80}\text{Fe}_{20}$.

This is a very interesting point because this mechanical behavior is totally concomitant with the objective of doing 1D or 2D nanostructuring to develop reliable flexible magnonic crystals. In order to address future objectives, the next paragraph will show some initial work in this direction.

III. PRELIMINARY RESULTS

A. Nanofabrication on flexible substrates

There are very few articles in the literature describing the development of magnetic nanostructures on flexible substrates.^{27,75} However, this is essential for the development of flexible magnetic

systems. A few recent works have been carried out using interference lithography (IL) and stencil lithography (SL) techniques.

IL is a mask-less nanofabrication technique, which has been used widely to synthesize large area magnetic nanostructures (see Fig. 4). The basic principle of IL involves the use of interference patterns generated from two obliquely incident beam paths (i.e., direct and reflected beams) to expose a photoresist layer.^{76,77} The patterned area and resolution are related to the beam source diameter and wavelength, respectively. The IL method allows multiple exposure steps to form a specific pattern on a resist. For example, in order to fabricate dot arrays, a second exposure after rotating the substrate through 90° is needed. The pitch resolution is linearly proportional to half the wavelength of the light and inversely proportional to the sine of the relative angle between the two beam paths. This technique has been used to fabricate a periodic array of magnetic nanostructures on polyethylene terephthalate⁷⁸ and Kapton.⁷⁹

A schematic showing the principle of interference lithography is presented in Fig. 4(a). To generate interference fringes on the surface of the photosensitive resin, the substrate is placed on an arm of Lloyd's mirror interferometer. The second arm of the interferometer contains a square aluminum mirror. The two arms of the interferometer are exposed to a continuous 325 nm beam generated by a Helium-Cadmium (He-Cd) laser ($\lambda = 325$ nm). The laser beam is focused through a lens into a 10 μm diameter hole, which helps eliminate noise and provides a Gaussian profile to the beam. After passing through this spatial filter, the beam propagates toward the sample. The light from the source beam interferes with

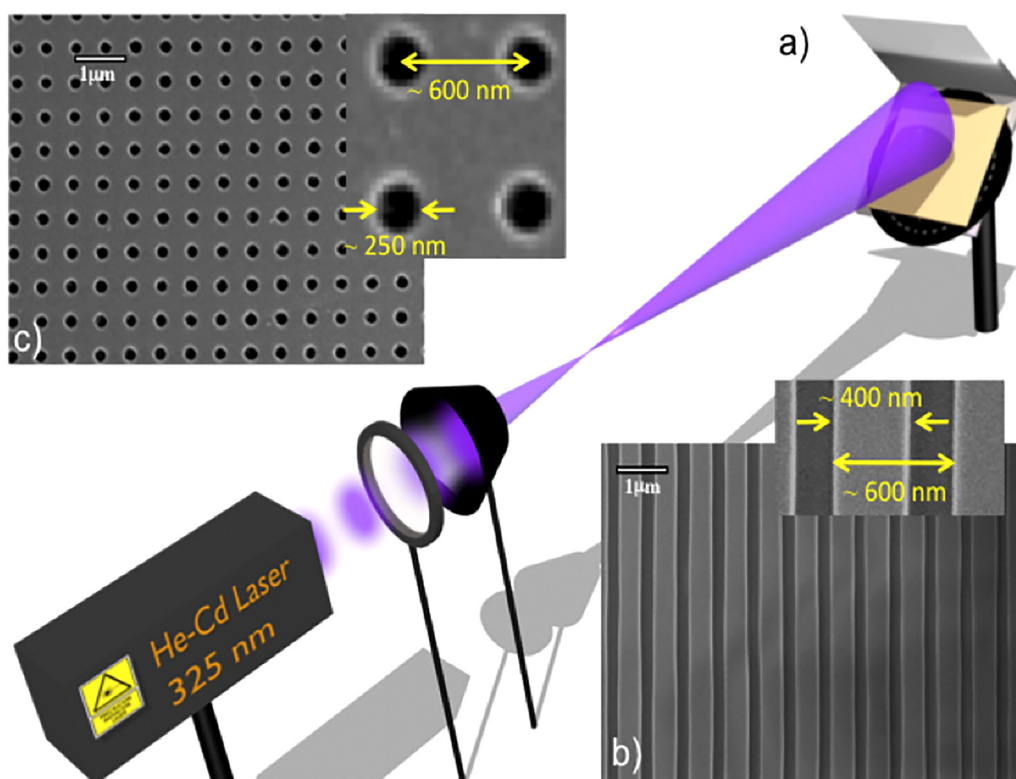


FIG. 4. (a) Schematic of the laser interference lithography setup showing the UV laser and Lloyd's mirror interferometer. (b) Scanning Electron Microscopy (SEM) image of an array of $\text{Ni}_{60}\text{Fe}_{40}$ nanowires (rectangular cross section) on the Kapton substrate fabricated using the IL process. The periodicity is around 600 nm with a nanowire width of about 400 nm. (c) SEM image of an array of $\text{Ni}_{60}\text{Fe}_{40}$ antidots on the Kapton substrate. The periodicity is around 600 nm with a hole diameter of about 250 nm.

the light reflected from the mirror to form a standing wave pattern with alternating maxima and minima of intensities. The periodicity of this alternation is equal to^{80–82}

$$p = \frac{\Lambda}{2 \sin \theta}.$$

It is proportional to the half-wavelength of the laser ($\Lambda/2$) and is inversely proportional to the sine of the relative angle θ of the two beams.⁸⁰ Figure 4(b) displays a typical scanning electron microscopy (SEM) image of the top surface of an array of $\text{Ni}_{80}\text{Fe}_{20}$ on a Kapton substrate fabricated using the IL process. The obtained periodicity is around 600 nm (nanowire width: 400 nm with an interspacing of 200 nm). Figure 4(c) shows antidot array $\text{Ni}_{60}\text{Fe}_{40}$ antidots on a Kapton substrate, and the periodicity is around 600 nm with a hole diameter of about 250 nm.

Nano-stencil lithography (SL) is a high-resolution shadow-mask nanofabrication technique used for patterning surfaces at the micro- and nanometer scales.^{83–86} It is a one-step technique that eliminates resist-related processing steps, which is common in a standard lithographic process. Actually, it is exactly the same principle used in prehistoric frescoes on which handprint paintings

have been found. Indeed, a stencil (membrane with apertures) is placed (aligned if necessary) and clamped to a substrate. The clamped set is placed in a deposition chamber where materials are evaporated through the stencil's apertures onto the substrate as illustrated in Figs. 5(a) and 5(b). SL is a very promising approach for synthesizing high quality magnetic nanostructures without using solvent and etching, thus reducing contamination sources. It is particularly useful for fabricating complex and multilayer nanostructures at an elevated temperature because no resist is involved.

Figure 5(c) presents an AFM image of an array of Co circular dots obtained thanks to the nano-stencil process. It corresponds to a square array with a periodicity of $2 \mu\text{m}$; the diameter of the dots is around $1 \mu\text{m}$. Figure 5(f) corresponds to a profile obtained from this image [white line in Fig. 5(d)] highlighting the periodicity and the thickness (100 nm) of this specific array. To conclude, Fig. 5(e) presents a 3D AFM image of four Co dots.

B. Magnetomechanical phenomena

Studies on the magnetomechanical properties of nanostructured arrays on flexible substrates are very rare. First, *in situ* magnetomechanical tests on $\text{Ni}_{60}\text{Fe}_{40}$ nanostructured arrays were proposed by Challab *et al.*⁷⁹ These nanowires deposited by IL on

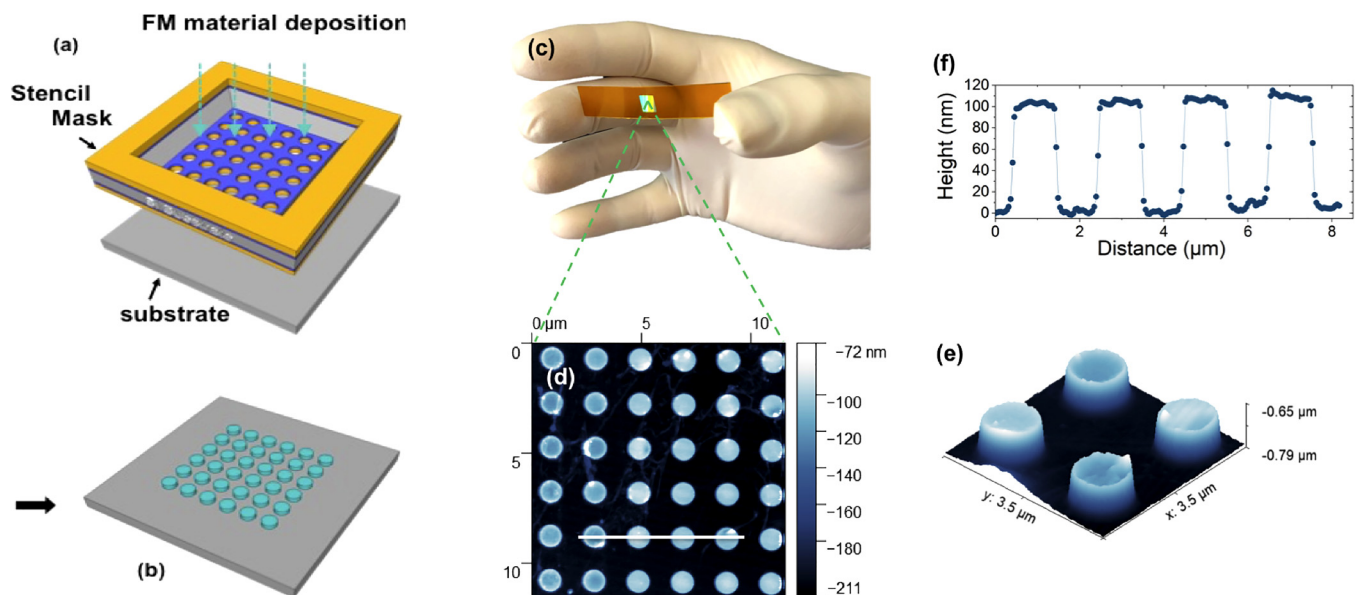


FIG. 5. Schematics of the stencil lithography process (a) and (b). For the sake of clarity, the pattern dimensions are exaggerated. The stencil mask consists of a rigid part supporting an Si_3N_4 membrane on which the desired pattern is etched. The e-beam deposition is performed through the stencil mask, which is then removed. Finally, an array of dots is obtained (b). (c) Kapton substrate with an array of Co nanodots, deposited by stencil lithography, at the center ($5 \times 5 \text{ mm}^2$ highlighted by a green color due to daylight diffraction), curved by the fingers of a human hand. (d) AFM image of a square array of Co circular dots fabricated using the nano-stencil process. The periodicity is around $2 \mu\text{m}$ with a dot diameter of about $1 \mu\text{m}$. (e) 3D AFM image of four Co dots. (f) Profile corresponding to the white line in image (c) highlighting a thickness of 100 nm for this array of dots.

Kapton were then cemented on a ferroelectric support, allowing to deform the magnetic system in its elastic domain (strains $< 0.1\%$); see Figs. 6(a) and 6(b).

The microwave properties could be measured *in situ* by micro-strip ferromagnetic resonance (MS-FMR) and Digital Image Correlation (DIC) techniques. MS-FMR was employed to probe the influence of the applied voltage on the magnetic properties via the resonance field of the uniform precession mode. The digital image correlation technique (DIC) was used to quantitatively measure the in-plane strains (ϵ_{xx} and ϵ_{yy}) of the ferroelectric actuator.⁸⁷ MS-FMR experiments allowed the resonance field probing by sweeping the applied magnetic field in the presence of a fixed pumping radio frequency (RF) field. In this kind of an RF-resonance technique, a weak modulation of the applied field ($\sim 2\text{--}5 \text{ Oe}$ at 1480 Hz) is performed in order to optimize the signal to noise ratio for a better lock-in detection of the signal. Thus, this technique gives access to the first field derivative of the RF absorption as a function of the applied field.⁸⁸ DIC is a technique that allows displacement and strain field measurements on an object surface by capturing images of the object surface at different states. One state is recorded before applying voltage, i.e., the reference image, and the other states are subsequent images of the deformed object. DIC generally uses random patterns of gray levels of the sample surface to measure the displacement via a correlation of a pair of digital images. Hence, from the measured strain fields, we can estimate the mean in-plane strains ϵ_{xx} and ϵ_{yy} , which cannot be straightforwardly attained with other techniques such as x-ray diffraction.

Figure 6(c) shows the resonance lines and, in particular, their shift when a strain state is applied (voltage applied to the ferroelectric substrate). On the one hand, the shift is different between a continuous thin film and nanowires of the same composition. On the other hand, depending on whether the positive strain is applied along the lines or perpendicular to the lines, the shift of the FMR lines is different. This is much more visible in Fig. 6(d), which shows this shift as a function of the voltage applied to the ferroelectric substrate. It can be seen that compared to the continuous $\text{Ni}_{60}\text{Fe}_{40}$ thin film, the lines strained positively parallelly follow a line shift of about 60% lower and about 50% lower for the nanowires strained positively perpendicularly.

In order to analyze these results, finite element calculations were performed to estimate the strain distribution in the system. Figures 6(a) and 6(b) show the strain map for the perpendicular and parallel configurations, respectively. It is clear that when a strain is applied along the length of the nanowires [ϵ_{yy} in Fig. 6(a), ϵ_{xx} in Fig. 6(b)], the strain is well transmitted from the substrate to the nanowires, while it is much less so for strain components perpendicular to these nanowires. This is due to the strong stiffness contrast between the magnetic nanowires and the polymer substrate in which the strains can be strongly concentrated in the case of interfaces not tangent to the applied forces. These analyses allowed us to propose a simple model of the magnetomechanical behavior of the system, including magnetoelastic effects and the true strain distribution. This allowed one to account very well for the experimental results, as can be seen in Fig. 6(d) (model is represented by the continuous lines).

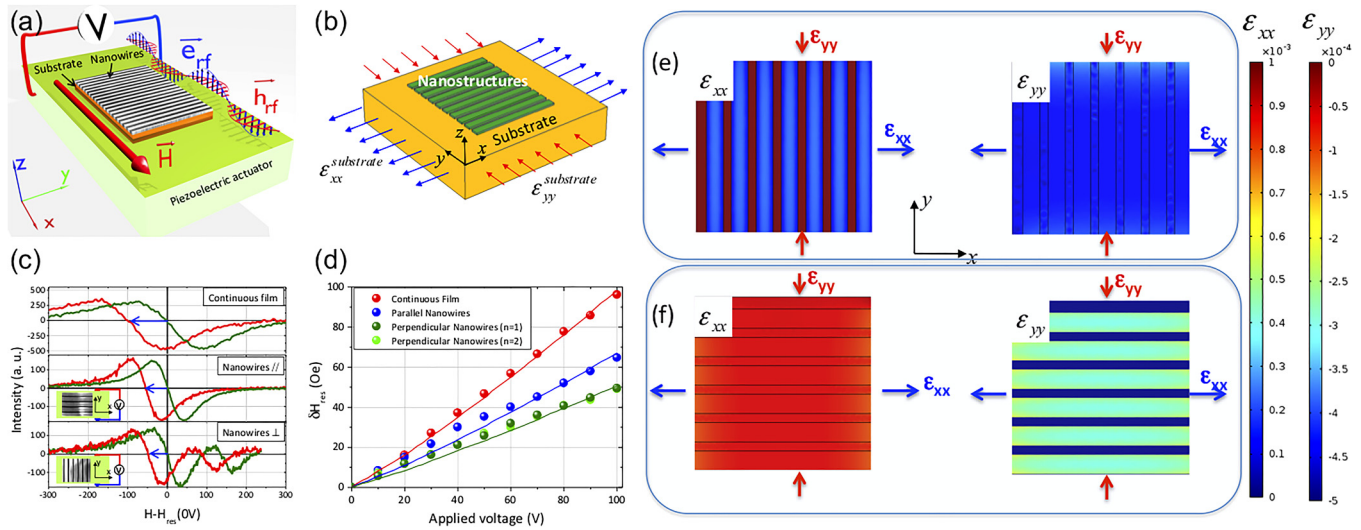


FIG. 6. (a) Schematic of an $\text{Ni}_{60}\text{Fe}_{40}$ nanowire array on a polymer substrate glued on the top of a ferroelectric actuator (green). \vec{H} corresponds to the applied magnetic field, while \vec{h}_r corresponds to the radiofrequency field. (b) Sketch of the system simulated by a finite element method (FEM). (c) Typical FMR spectra obtained in presence at 0 and 100 V for three different systems. (d) Resonance field shift δH_{res} variation as a function of the applied voltage for the three different systems [see (b)]. Symbols represent experimental data, while full lines are obtained by numerical calculations. The experiments are simulated by introducing the calculated strains (FEM) in the Landau–Lifshitz–Gilbert equation. (e) and (f) In-plane strain maps of the calculated in-plane strains when ϵ_{xx} is either perpendicular (a) or parallel (b) to the nanowires. Adapted with permission from Challab *et al.*, Phys. Status Solidi Rapid Res. Lett. **13**, 1800509 (2019). Copyright 2019 John Wiley & Sons.

If these observations are now extrapolated to more extreme cases, it is imaginable to build nanoarchitectures of magnetic materials for which the strain control of magnetic properties is total and others on the contrary for which the nanostructures deform very little despite a large amount of strain in the substrate. This allows us to envisage several possible applications for the strain control of properties or the insensitivity of the properties to the substrate strains.

IV. FUTURE STRATEGY AND PERSPECTIVES

A. Magnetomechanical properties

We know that the geometry of nanostructures is a key factor shown in Fig. 6 from Challab *et al.*⁷⁹ This figure, based on numerical calculations, shows several interesting points: for a substrate subjected to strain, the strain transmission from the substrate to the adherent nanostructures on the surface depends very much on the aspect ratio (thickness/width, with a typical width of a few hundred nm) of these nanostructures. Thin thicknesses (a few nm) favor a good strain transmission (because the local stiffening is quite low), while thicker thicknesses (hundreds of nanometers) stiffen locally enough to make the strains tend toward zero in the nanostructures. This phenomenon depends strongly on the rigidity of the substrate. What is said above is true for Kapton, which is quite rigid for a polymer (Young's modulus = 4 GPa). Thus, this substrate allows, for small thicknesses of nanostructures, a significant strain transmission. This can be interesting for sensor applications because it is possible to control the magnonic bands by magnetoelastic coupling via the strains in the nanostructures. However, for greater

thicknesses, applications requiring stability of microwave properties at large external strains can be envisaged.

Thus, both types of applications can be considered: tailoring the properties with strain at a low aspect ratio for magnetization strain control applications (flexible devices), keeping constant the properties with strain for highly stretchable devices. Considering the control of properties by bending, many works have been made for continuous thin films for sensing applications.^{89,90} In the future, this same concept could be applied to magnonic systems in order to modulate their band properties by applying small controlled strains [which is the case of bending (a few %)]. This will be discussed in Sec. IV C.

The concept of insensitivity to strains has been proposed more recently by Shen *et al.*, not in the context of magnonic crystals, but using dispersed LaFeO_3 nanowires on a flexible MICA substrate.²² Obviously, the non-periodic character does not allow for band structures, but they showed that for a fairly long aspect ratio, the microwave properties of the system did not depend on the curvature of the system due to the strain localization effects that Challab *et al.* quantified.⁷⁹ Muscas *et al.* also showed a weak magnetomechanical effect in cobalt nanowires deposited periodically on flexible PEN substrates; see Fig. 7(a).⁹¹ A very little variation in static magnetic properties as a function of substrate curvature is shown in this article. Muscas *et al.* analyzed this as weakening of the magnetostriction coefficient of cobalt in a nanowire form, but it is more likely that this effect is due to low strain concentrations in the nanowires. This is because the bending imposed on the substrate is applied perpendicular to the nanowires, as shown in Fig. 7(b), which tends to concentrate the strains in the flexible substrate,

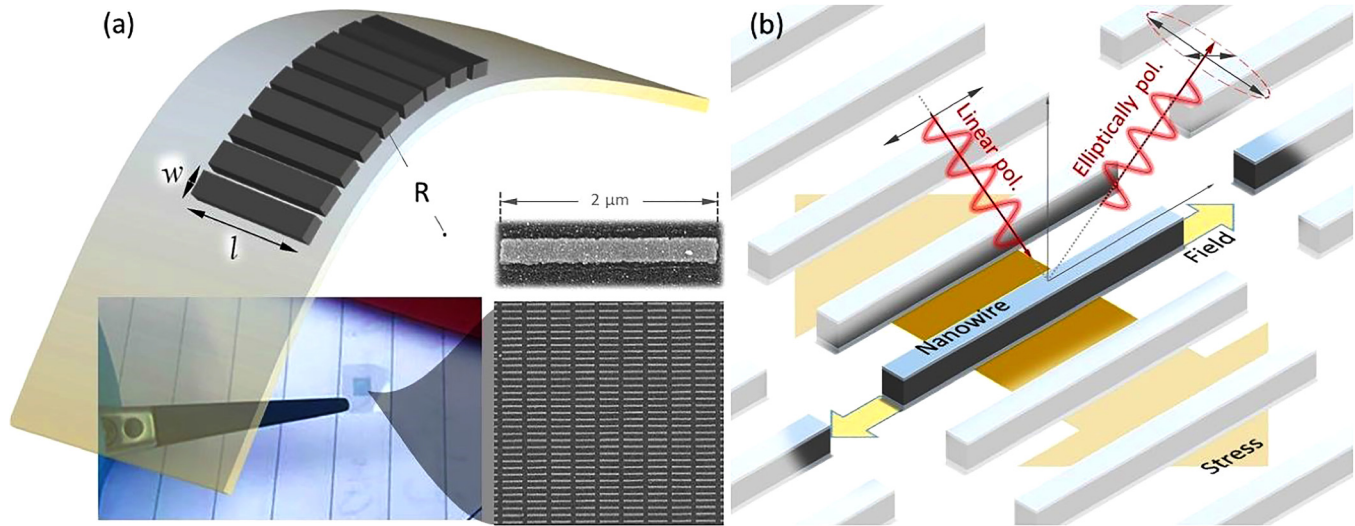


FIG. 7. (a) Images showing nanowires ($0.2 \times 2 \mu\text{m}^2$) on a polymer [polyethylene naphthalate (PEN)] substrate. (b) Sketch showing the stress axis that is perpendicular to the nanowire length (and to the applied magnetic field). Adapted with permission from Muscas *et al.*, *Nanoscale* **13**, 6043 (2021). Copyright 2021 The Royal Society of Chemistry.

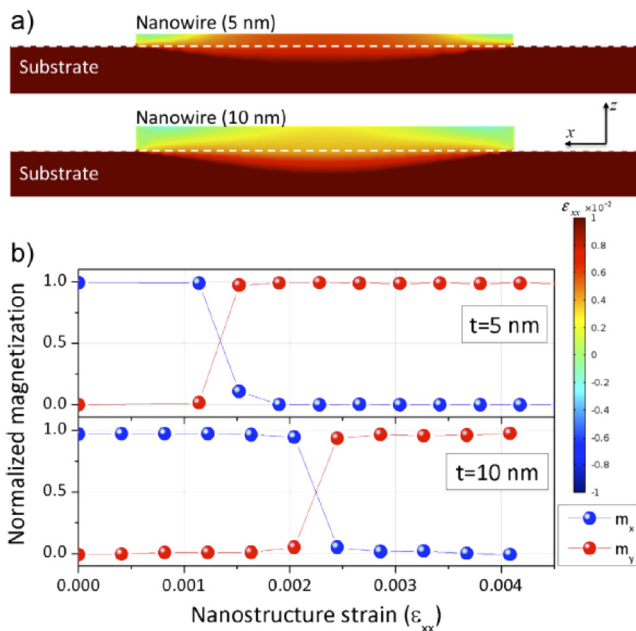


FIG. 8. (a) 2D maps of ϵ_{xx} in a cross section made at the center of each nanowire for a substrate displacement equal to 3 nm on both extremities of the substrate. (b) Evolution of the mean values of the normalized magnetization components (m_x and m_y) as a function of the mean x-component strain ϵ_{xx} inside the substrate for two different values (5 and 10 nm) of the nanowire thickness. Reproduced with permission from Challab *et al.*, *J. Phys. D: Appl. Phys.* **52**, 355004 (2019). Copyright 2019 IOP Publishing LLC.

as shown by Challab *et al.*⁷⁹ This work confirms that development of nanostructure arrays on flexible substrates can be a very relevant way for creating magnetic systems insensitive to external strains.

B. Modeling

Modeling the properties of magnonic crystals involves the use of software making it possible to numerically solve the Landau–Lifshitz–Gilbert (LLG) equation. Indeed, when studying such crystal properties, it is only possible to obtain an analytical expression for spin-wave dispersions at the cost of approximations, which are sometimes too unrealistic. Indeed, in the case of magnetic objects whose dimensionality is reduced, new free surfaces appear and give rise to heterogeneous demagnetizing fields, which *in fine* are too complex to be analytically calculated. By cleverly using the most commonly micromagnetic softwares (OOMMF,⁹² Mumax³,⁹³ Nmag,⁹⁴ Finmag,⁹⁵ ...), it is possible to determine the spin-wave dispersions in such magnonic crystals.^{96–99} However, none of these codes is coupled to the equations of solid mechanics, and none of them allows one to determine heterogeneous strain fields and to take them into account when solving the LLG equation. For magnonic crystals on flexible substrates, it is important to include local strains in the problem because heterogeneities can be strong and influence the micromagnetic behavior. The magnetoelastic coupling (magnetization, strain, and their coupling) must, therefore, be fully described at the local scale. A few groups have implemented numerical codes that couple the LLG equation describing the magnetization dynamics as well as the solid mechanics ones in strain-mediated artificial multiferroics.^{100–102} These codes could be very well adapted to the problem of systems with flexible substrates.

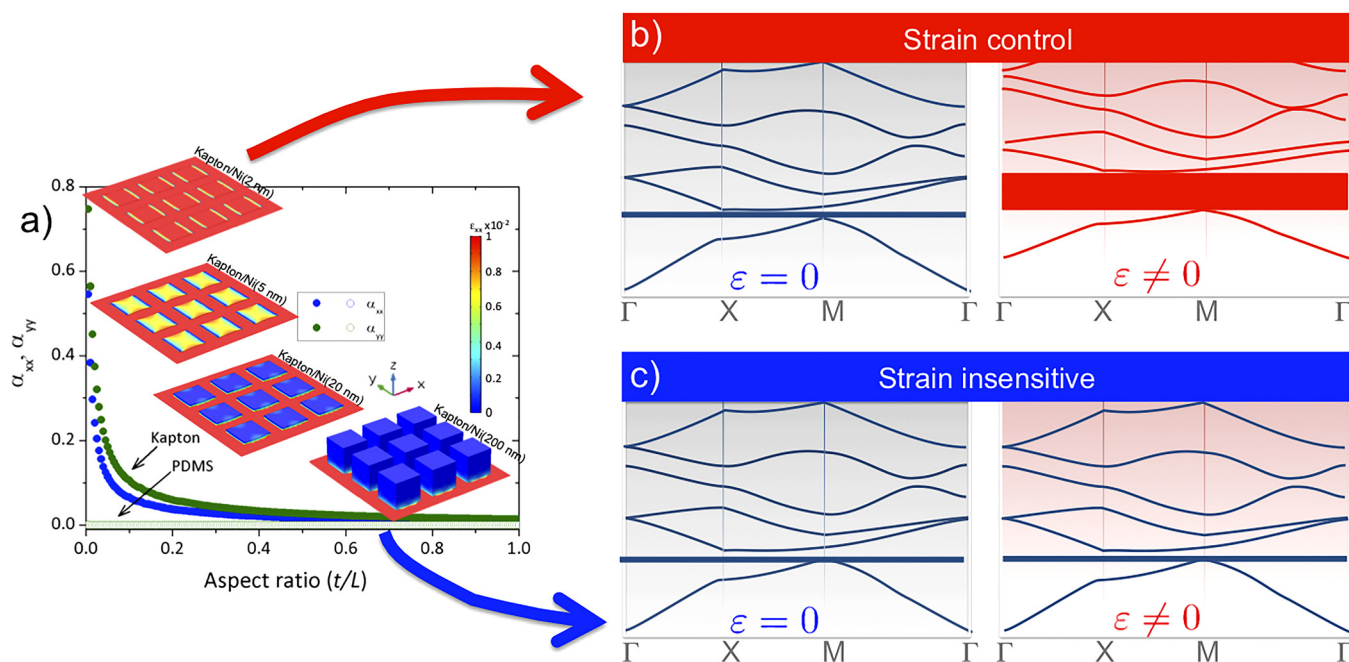


FIG. 9. (a) In-plane strain transmission rate of a metallic nanodot/polymer substrate system as a function of the nanodot aspect ratio. (b) and (c) Concept demonstration showing the magnonic bands of a square 2D crystal (Γ , X , and M correspond to the high symmetry points of the first Brillouin zone) in the absence and presence of applied strains (ϵ). Strain control (b) is attained for low aspect ratio systems, and strain insensitivity (c) is obtained at a higher aspect ratio (depending on the stiffness contrast between the nanostructures and the substrate). The blue and red bands illustrate the evolution (or not) of the mean position and width of a magnonic bandgap. Obviously, differences in the magnonic band energies and oscillations must appear depending on whether the aspect ratio of the magnonic crystal is small or large, but this is a very schematic representation that highlights the concept of strain control or strain insensitivity of the magnonic properties.

In this context, a numerical simulation tool that accounts for the heterogeneous strain fields of magnetic deformable objects has been developed by Challab *et al.*,¹⁰³ validated and tested for nanostructures on a compliant substrate. The LLG equation was solved by finite element methods in a fully coupled way with solid mechanical governing equations and the resolution was achieved within the software COMSOL Multiphysics.¹⁰⁴ The simulation tool has been deployed in order to examine the effect of the nanowire thickness on the magnetoelastic behavior of a hybrid material system (magnetic nanowire on a polymer substrate). It was found that the strain transmitted from the substrate to the nanostructure changes with the thickness, regarding its distribution and mean value, and thus induces different magnetoelastic fields. In addition, it was found that the thickness influences the shape anisotropy and renders more complex the outcome of the competition with magnetoelastic anisotropy. 2D maps of the strain ϵ_{xx} in a cross section made at the center of each nanowire (for a displacement equal to 3 nm) are reported in Fig. 8(a). It is clearly shown from this figure that the transmitted strain to the nanowire is heterogeneous for both values of the thickness. For the two different values of the nanowire thickness, the strain transmitted from the substrate to the nanostructure is sufficiently high to make rotate the equilibrium magnetization; i.e., the magnetoelastic energy compensates the shape anisotropy one, and this value depends strongly on the applied strain [Fig. 8(b)].

The next step to describe a magnonic crystal is now to describe a complete network of nanostructures undergoing these heterogeneities and to calculate the corresponding dispersion relation. There are still unknown effects because the free edges play a dominant role in the inhomogeneity of the magnetoelastic field. This model would allow us to anticipate the arrays to be developed experimentally to approach the desired magnonic properties.

C. Magnonic band structure under strains

Concerning precisely the magnonic crystals on a flexible substrate, no work has so far shown the evolution of a magnonic band structure with external strains. However, we can consider two extreme cases as shown in Fig. 9. Figure 9(a) reminds the work of Challab *et al.*,⁷⁹ which shows that the strain transmission (α_{xx} and α_{yy}) depends strongly on the aspect ratio of the nanostructures for a given stiffness contrast between the nanostructures and the substrate. Thus, it is quite straightforward to design the concept of a band structure that can be strain-controlled via magnetoelastic coupling for low aspect ratios or strain-insensitive at higher aspect ratios. We show in Fig. 9 a concept demonstration (i.e., strain control for a low aspect ratio and strain-insensitivity for a high aspect ratio) on a fictitious 2D-square magnonic crystal, which is represented here through the projection of its magnonic bands along the high symmetry points of the first Brillouin zone.^{105–107}

Figure 9(b) shows schematically the control of the magnonic bands by applying a controlled strain. Like the controllability by an external magnetic field, a magnetoelastic field will allow to vary both the average position of the bands and their width. For small strains (such as by bending, a few %), it is possible to vary position and width in the GHz range in the absence of a magnetic field. This has not yet been reported in the literature.

Figure 9(c) concerns the other extreme case for which the strain transmission is too small (and, therefore, the magnetoelastic field) to vary the magnonic bands. This is the case of high aspect ratio nanostructures. This concept can be applied to systems subjected to strong strains (stretchable, a few 10%) for which one wishes a good stability/durability of the magnonic properties. It should be noted that the durability of continuous thin film magnetic systems is extremely difficult to achieve (often early appearance of cracks) and that this solution is more general than magnonics alone.

The perspectives to these extreme behaviors are numerous, and possibilities can be explored between them. Indeed, depending on the geometry of the nanostructures, strain heterogeneity can be significant in individual nanostructures because of free surfaces (see Fig. 8). In this case, different magnetic modes do not feel the same magnetoelastic field, which will lead to a differentiated tunability of the magnonic bands depending on the spatial localization of spin-wave modes in each nanostructure. This property has been proposed very recently by Challab *et al.* who show that the application of a weak strain to an $\text{Ni}_{60}\text{Fe}_{40}$ antidot system leads to a differentiated variation of spin wave energy of several tens of %.¹⁰⁸ This position-dependent tunability is a possibility that is difficult to offer with an external magnetic field applied to an array of same nanostructures. As an extension, one can imagine assemblies of nanostructures with different lateral geometries (isotropic or anisotropic), or even of different thicknesses, which offer a multitude of very different strain fields from one type of nanostructure to another. Thus, magnonic systems on polymer substrates can exhibit high modulability due to the strong dependence of the strain field with the aspect ratio. For example, bicomponent magnonic crystals can be constituted by nanostructures that alternatively deform or not. This approach can be very complementary to 3D magnonics as proposed in Gubiotti *et al.*¹⁰⁹ Indeed, meander structures allow them to play on the dipolar coupling and thus the dispersion relation of the spin waves. It is possible to create meandering structures on a polymer substrate. These could be continuous as in Giubotti *et al.* or slightly discontinuous in order to create free surfaces to induce additional strain heterogeneities. This further increases the number of possible studies. The exploitation of these concepts may allow one to extend the existing applications of magnonic systems by taking advantage of compliant substrates. These developments are to be compared with the complementary ones in curvilinear magnonics,¹¹⁰ which propose new magnetic objects with highly complex geometries (curved wires^{111,112} or 3D nanovolcanoes¹¹³) in order to reveal induced phenomena such as the confinement of magnetic modes for applications in multimode microwave resonators.¹¹⁰

V. CONCLUSION

To conclude, this paper shows that flexible magnetic systems can benefit from periodic nanostructuring and its associated

properties. From a magnetic property point of view, this periodic nature allows one to consider the development of flexible magnonic crystals for applications in high frequency devices. Another important point is the influence of the geometrical parameters of the nanostructured arrays on the mechanical properties of these systems. This Perspective shows that geometrical tuning can significantly modify the strain transfer from the substrate to the nanostructures. It is thus possible to produce systems whose properties can be varied by the strains to different degrees. It is even possible to create flexible magnonic crystals insensitive to strains with increased durability. This large set of possibilities is thus very promising for the applicability of high frequency systems conformable to non-planar surfaces.

ACKNOWLEDGMENTS

The authors would like to thank Université Sorbonne Paris Cité and the National University of Singapore for their support through the USPC-NUS program (MagnoFlex project, No. ANR-11-IDEX-0005-02 and Nanoflex project, No. 2016-04-R/USPC-NUS). D.F. and F.Z. would like to thank Labex SEAM (Science and Engineering for Advanced Materials and devices) for financial support through the MECAMAG project (Nos. ANR-10-LABX-0096 and ANR-18-IDEX-0001). The research was conducted within the context of the CNRS-NUS International Research Project “Heterogeneous stretchable systems, mechanical properties and associated functionalities at small scales”—StretchSmart.

AUTHOR DECLARATIONS

Conflict of Interest

The authors have no conflicts to disclose.

DATA AVAILABILITY

The data that support the findings of this study are available from the corresponding author upon reasonable request.

REFERENCES

- ¹G. Lin, D. Makarov, M. Melzer, W. Si, C. Yan, and O. G. Schmidt, *Lab Chip* **14**, 4050 (2014).
- ²S. Kim, H. Y. Jeong, S. K. Kim, S.-Y. Choi, and K. J. Lee, *Nano Lett.* **11**, 5438 (2011).
- ³M. Kaltenbrunner, M. S. White, E. D. Glowacki, T. Sekitani, T. Someya, N. S. Sariciftci, and S. Bauer, *Nat. Commun.* **3**, 770 (2012).
- ⁴L. Li, J. Liang, S. Y. Chou, X. Niu, Z. Yu, and Q. Pei, *Sci. Rep.* **4**, 4307 (2014).
- ⁵S. Das, R. Gulotty, A. V. Sumant, and A. Roelofs, *Nano Lett.* **14**, 2861–2866 (2014).
- ⁶S. Wang, J. Xu, W. Wang, G.-J. Nathan Wang, R. Rastak, F. Molina-Lopez, J. W. Chung, S. Niu, V. R. Feig, J. Lopez, T. Lei, S.-K. Kwon, Y. Kim, A. M. Foudeh, A. Ehrlich, A. Gasperini, Y. Yun, B. Murmann, J. B.-H. Tok, and Z. Bao, *Nature* **555**, 83 (2018).
- ⁷Q. Hua, J. Sun, H. Liu, R. Bao, R. Yu, J. Zhai, C. Pan, and Z. L. Wang, *Nat. Commun.* **9**, 244 (2018).
- ⁸W. Gao, H. Ota, D. Kiriya, K. Takei, and A. Javey, *Acc. Chem. Res.* **52**(3), 1203 (2019).
- ⁹K. J. Yu, Z. Yan, M. Han, and J. A. Rogers, *npj Flex. Electron.* **1**, 4 (2017).
- ¹⁰Y. Yang and W. Gao, *Chem. Soc. Rev.* **48**, 1465 (2019).
- ¹¹M. Stoppa and A. Chiolerio, *Sensors* **14**, 11957 (2014).

- ¹²N. Matsuhisa, M. Kaltenbrunner, T. Yokota, H. Jinno, K. Kuribara, T. Sekitani, and T. Someya, *Nat. Commun.* **6**, 7461 (2015).
- ¹³H. M. Lee, S.-Y. Choi, A. Jung, and A. H. Ko, *Angew. Chem.* **125**, 7872 (2013).
- ¹⁴Y. Chen, J. Au, P. Kazlas, A. Ritenour, H. Gates, and M. McCreary, *Nature* **423**, 136 (2003).
- ¹⁵D. R. Cairns and G. P. Crawford, *Proc. IEEE* **93**, 1451 (2005).
- ¹⁶M.-C. Choi, Y. Kim, and C.-S. Ha, *Prog. Polym. Sci.* **33**, 581 (2008).
- ¹⁷G. S. C. Bermúdez and D. Makarov, *Adv. Funct. Mater.* **31**, 2007788 (2021).
- ¹⁸A. Bedoya-Pinto, M. Donolato, M. Gobbi, L. E. Hueso, and P. Vavassori, *Appl. Phys. Lett.* **104**, 062412 (2014).
- ¹⁹M. Kondo, M. Melzer, D. Karnaushenko, T. Uemura, S. Yoshimoto, M. Akiyama, Y. Noda, T. Araki, O. G. Schmidt, and T. Sekitani, *Sci. Adv.* **6**, eaay6094 (2020).
- ²⁰M. Ha, G. S. C. Bermúdez, T. Kosub, I. Mönch, Y. Zabala, E. S. O. Mata, R. Illing, Y. Wang, J. Fassbender, and D. Makarov, *Adv. Mater.* **33**, 2005521 (2021).
- ²¹S. Zhao, Z. Zhou, C. Li, B. Peng, Z. Hu, and M. Liu, *ACS Nano* **12**, 7167 (2018).
- ²²L. Shen, G. Lan, L. Lu, C. Ma, C. Cao, C. Jiang, H. Fu, C. You, X. Lu, Y. Yang, L. Chen, M. Liu, and C.-L. Jia, *Adv. Sci.* **5**, 1800855 (2018).
- ²³M. Donolato, C. Tollan, J. M. Porro, A. Berger, and P. Vavassori, *Adv. Mater.* **25**, 623–629 (2013).
- ²⁴D. Makarov, M. Melzer, D. Karnaushenko, and O. G. Schmidt, *Appl. Phys. Rev.* **3**, 011101 (2016).
- ²⁵O. Lee, L. You, J. Jang, V. Subramanian, and S. Salahuddin, *Appl. Phys. Lett.* **107**, 252401 (2015).
- ²⁶B. Li, M. N. Kavalzhiev, and J. Kosel, *J. Magn. Magn. Mater.* **378**, 499 (2015).
- ²⁷F. Zighem, D. Faurie, M. Belmeguenai, A. Garcia-Sanchez, P. Lupo, and A. O. Adeyeye, *Appl. Phys. Lett.* **111**, 052408 (2017).
- ²⁸K. Zakeri, *J. Phys.: Condens. Matter* **32**, 363001 (2020).
- ²⁹A. V. Chumak, A. A. Serga, and B. Hillebrands, *J. Phys. D: Appl. Phys.* **50**, 244001 (2017).
- ³⁰S. Neusser and D. Grundler, *Adv. Mater.* **21**, 2927 (2009).
- ³¹K.-S. Lee, D.-S. Han, and S.-K. Kim, *Phys. Rev. Lett.* **102**, 127202 (2009).
- ³²G. Gubbiotti, M. Kostylev, S. Tacchi, M. Madami, G. Carlotti, J. Ding, A. O. Adeyeye, F. Zighem, A. A. Stashkevich, E. Ivanov, and S. Samarin, *J. Phys. D: Appl. Phys.* **47**, 105003 (2014).
- ³³Z. K. Wang, V. L. Zhang, H. S. Lim, S. C. Ng, M. H. Kuok, S. Jain, and A. O. Adeyeye, *ACS Nano* **4**, 643 (2010).
- ³⁴G. Gubbiotti, S. Tacchi, M. Madami, G. Carlotti, A. O. Adeyeye, and M. Kostylev, *J. Phys. D: Appl. Phys.* **43**, 264003 (2010).
- ³⁵A. Khitun, M. Bao, and K. L. Wang, *J. Phys. D: Appl. Phys.* **43**, 264005 (2010).
- ³⁶J. Ding, M. P. Kostylev, and A. O. Adeyeye, *Appl. Phys. Lett.* **100**, 073114 (2012).
- ³⁷D. Apalkov, B. Dieny, and J. M. Slaughter, *Proc. IEEE* **104**, 1796 (2016).
- ³⁸S. Tsunashima, *J. Phys. D: Appl. Phys.* **34**, R87 (2001).
- ³⁹S. Geiger, J. Michon, S. Liu, J. Qin, J. Ni, J. Hu, T. Gu, and N. Lu, *ACS Photonics* **7**, 2618 (2020).
- ⁴⁰G. C. Righini, J. Krzak, A. Lukowiak, G. Macrelli, S. Varas, and M. Ferrari, *Opt. Mater.* **115**, 111011 (2021).
- ⁴¹S. Kumari, S. Mohapatra, and R. S. Moirangthem, *Mater. Today: Proc.* **5**, 2216 (2018).
- ⁴²P. Jia, D. Kong, and H. Ebendorff-Heidepriem, *ACS Appl. Nano Mater.* **3**, 8242 (2020).
- ⁴³D. Grundler, *Nat. Phys.* **11**, 438 (2015).
- ⁴⁴J. Ding, M. Kostylev, and A. O. Adeyeye, *Phys. Rev. Lett.* **107**, 047205 (2011).
- ⁴⁵A. Haldar, D. Kumar, and A. O. Adeyeye, *Nat. Nanotechnol.* **11**, 437 (2016).
- ⁴⁶M. Krawczyk and D. Grundler, *J. Phys.: Condens. Matter* **26**, 123202 (2014).
- ⁴⁷S. P. Lacour, D. Chan, and S. Wagner, *Appl. Phys. Lett.* **88**, 204103 (2006).
- ⁴⁸A. V. Sadvonnikov, V. A. Gubanov, S. E. Sheshukova, Y. P. Sharaevskii, and S. A. Nikitov, *Phys. Rev. Appl.* **9**, 051002 (2018).
- ⁴⁹S. Klingler, P. Pirro, T. Brächer, B. Leven, B. Hillebrands, and A. V. Chumak, *Appl. Phys. Lett.* **106**, 212406 (2015).
- ⁵⁰A. Khitun, *J. Appl. Phys.* **111**, 054307 (2012).
- ⁵¹A. Haldar and A. O. Adeyeye, *J. Appl. Phys.* **128**, 240902 (2020).
- ⁵²M. Krawczyk and H. Puzskarski, *Phys. Rev. B* **77**, 054437 (2008).
- ⁵³G. Gubbiotti, S. Tacchi, G. Carlotti, N. Singh, S. Goolaup, A. O. Adeyeye, and M. Kostylev, *Appl. Phys. Lett.* **90**, 092503 (2007).
- ⁵⁴M. Kostylev, P. Schrader, R. L. Stamps, G. Gubbiotti, G. Carlotti, A. O. Adeyeye, S. Goolaup, and N. Singh, *Appl. Phys. Lett.* **92**, 132504 (2008).
- ⁵⁵Z. K. Wang, V. L. Zhang, H. S. Lim, S. C. Ng, M. H. Kuok, S. Jain, and A. O. Adeyeye, *Appl. Phys. Lett.* **94**, 083112 (2009).
- ⁵⁶J. Ding and A. O. Adeyeye, *Adv. Funct. Mater.* **23**, 1684 (2013).
- ⁵⁷S. Tacchi, F. Montoncello, M. Madami, G. Gubbiotti, G. Carlotti, L. Giovannini, R. Zivieri, F. Nizzoli, S. Jain, A. O. Adeyeye, and N. Singh, *Phys. Rev. Lett.* **107**, 127204 (2011).
- ⁵⁸S. Tacchi, G. Gubbiotti, M. Madami, and G. Carlotti, *J. Phys.: Condens. Matter* **29**, 073001 (2016).
- ⁵⁹S. O. Demokritov and A. N. Slavin, *Magnonics: From Fundamentals to Applications* (Springer, 2013).
- ⁶⁰S. Gliga, E. Iacocca, and O. G. Heinonen, *APL Mater.* **8**, 040911 (2020).
- ⁶¹M. Melzer, D. Makarov, A. Calvimontes, D. Karnaushenko, S. Baunack, R. Kaltofen, Y. Mei, and O. G. Schmidt, *Nano Lett.* **11**, 2522 (2011).
- ⁶²M. Melzer, M. Kaltenbrunner, D. Makarov, D. Karnaushenko, D. Karnaushenko, T. Sekitani, T. Someya, and O. G. Schmidt, *Nat. Commun.* **6**, 6080 (2015).
- ⁶³P. Sheng, B. Wang, and R.-W. Li, *J. Semicond.* **39**, 011006 (2018).
- ⁶⁴R. U. R. Sagar, M. Galluzzi, A. García-Peñas, M. A. Bhat, and M. Z. F. J. Stadler, *Nano Res.* **12**, 101 (2019).
- ⁶⁵S.-Y. Cai, C.-H. Chang, H.-I. Lin, Y.-F. Huang, W.-J. Lin, S.-Y. Lin, Y.-R. Liou, T.-L. Shen, Y.-H. Huang, P.-W. Tsao, C.-Y. Tzou, Y.-M. Liao, and Y.-F. Chen, *ACS Appl. Mater. Interfaces* **10**, 17393 (2018).
- ⁶⁶T. Uhrmann, L. Bär, T. Dimopoulos, N. Wiese, M. Rührig, and A. Lechner, *J. Magn. Magn. Mater.* **307**, 209 (2006).
- ⁶⁷Y.-F. Chen, Y. Mei, R. Kaltofen, J. I. Mönch, J. Schumann, J. Freudenberger, H.-J. Klauß, and O. G. Schmidt, *Adv. Mater.* **20**, 3224 (2008).
- ⁶⁸B. Özkaya, S. R. Saranu, S. Mohanan, and U. Herr, *Phys. Status Solidi A* **205**, 1876 (2008).
- ⁶⁹M. Melzer, M. Kaltenbrunner, D. Makarov, D. Karnaushenko, D. Karnaushenko, T. Sekitani, T. Someya, and O. G. Schmidt, *Nat. Commun.* **6**, 6080 (2015).
- ⁷⁰M. Melzer, D. Makarov, and O. G. Schmidt, *J. Phys. D: Appl. Phys.* **53**, 083002 (2019).
- ⁷¹M. Melzer, G. Lin, D. Makarov, and O. G. Schmidt, *Adv. Mater.* **24**, 6468 (2012).
- ⁷²S. Merabtine, F. Zighem, A. Garcia-Sanchez, V. Gunasekaran, M. Belmeguenai, X. Zhou, P. Lupo, A. O. Adeyeye, and D. Faurie, *Sci. Rep.* **8**, 13695 (2018).
- ⁷³M. Melzer, D. Karnaushenko, G. Lin, S. Baunack, D. Makarov, and O. G. Schmidt, *Adv. Mater.* **27**, 1333 (2015).
- ⁷⁴H. Li, Q. Zhan, Y. Liu, L. Liu, H. Yang, Z. Zuo, T. Shang, B. Wang, and R.-W. Li, *ACS Nano* **10**, 4403 (2016).
- ⁷⁵S. Merabtine, F. Zighem, D. Faurie, A. Garcia-Sanchez, P. Lupo, and A. Adeyeye, *Nano Lett.* **18**, 3199 (2018).
- ⁷⁶C. Lu and R. H. Lipson, *Laser Photon. Rev.* **4**, 568 (2010).
- ⁷⁷M. Maldovan and E. L. Thomas, *Periodic Materials and Interference Lithography: For Photonics, Phononics and Mechanics* (Wiley-VCH Verlag GmbH & Co. KGaA, 2009).
- ⁷⁸B. H. Li, X. Liu, M. Zhu, Z. Wang, A. O. Adeyeye, and W. K. Choi, *J. Nanosci. Nanotechnol.* **15**, 4332 (2015).
- ⁷⁹N. Challab, F. Zighem, D. Faurie, M. Haboussi, M. Belmeguenai, P. Lupo, and A. O. Adeyeye, *Phys. Status Solidi Rapid Res. Lett.* **13**, 1800509 (2019).
- ⁸⁰H. V. Wolferen and L. Abelmann, “Laser interference lithography,” in *Lithography: Principles, Processes and Materials*, edited by T. C. Hennessy (Nova Science Publishers, Inc., 2011), pp. 133–148, ISBN: 978-1-61761-837-6.

- ⁸¹J. D. Boor, N. Geyer, J. V. Wittemann, U. Gösele, and V. Schmidt, *Nanotechnology* **21**, 095302 (2010).
- ⁸²J.-H. Seo, J. H. Park, S.-I. Kim, B. J. Park, Z. Mal, J. Choi, and B.-K. Ju, *J. Nanosci. Nanotechnol.* **14**, 1521 (2014).
- ⁸³J. Arcamone, M. A. F. van den Boogaart, F. Serra-Graells, J. Fraxedas, J. Brugger, and F. Pérez-Murano, *Nanotechnology* **19**, 305302 (2008).
- ⁸⁴S. Aksu, A. E. Cetin, R. Adato, and H. Altug, *Adv. Opt. Mater.* **1**, 798 (2013).
- ⁸⁵F. Yesilkoy, V. Flauraud, M. Rüegg, B. J. Kimb, and J. Brugger, *Nanoscale* **8**, 4945 (2016).
- ⁸⁶O. Vazquez-Mena, L. Gross, S. Xie, L. G. Villanueva, and J. Brugger, *Microelectron. Eng.* **132**, 236 (2015).
- ⁸⁷F. Zighem, M. Belmeguenai, D. Faurie, H. Haddadi, and J. Moulin, *Rev. Sci. Instrum.* **85**, 103905 (2014).
- ⁸⁸M. Gueye, F. Zighem, M. Belmeguenai, M. Gabor, C. Tiusan, and D. Faurie, *J. Phys. D: Appl. Phys.* **49**, 265001 (2016).
- ⁸⁹M. Gueye, B. M. Wague, F. Zighem, M. Belmeguenai, M. S. Gabor, T. Petrisor, Jr., C. Tiusan, S. Mercone, and D. Faurie, *Appl. Phys. Lett.* **105**, 062409 (2014).
- ⁹⁰Y. Zhang, L. Shen, M. Liu, X. Li, X. Lu, L. Lu, C. Ma, C. You, A. ChenO, C. Huang, L. Chen, M. Alexe, and C.-L. Jia, *ACS Nano* **11**, 8002 (2017).
- ⁹¹G. Muscas, P. E. Jönsson, I. G. Serrano, Ö. Vallin, and M. V. Kamalakar, *Nanoscale* **13**, 6043 (2021).
- ⁹²M. J. Donahue, OOMMF User's Guide, version 1.0, Interagency Report NISTIR 6376, NIST, Gaithersburg, MD, 1999.
- ⁹³A. Vansteenkiste, J. Leliaert, M. Dvornik, M. Helsen, F. Garcia-Sanchez, and B. Van Waeyenberge, *AIP Adv.* **4**, 107133 (2014).
- ⁹⁴T. Fischbacher, M. Franchin, G. Bordignon, and H. Fangohr, *IEEE Trans. Magn.* **43**, 2896 (2007).
- ⁹⁵M.-A. Bisotti, M. Beg, W. Wang, M. Albert, D. Chernyshenko, D. Cortés-Ortuño, R. A. Pepper, M. Vousden, R. Carey, H. Fuchs, A. Johansen, G. Balaban, L. Breth, T. Kluyver, and H. Fangohr, see <https://zenodo.org/record/1216011#.YWaV4NMzaHo> for "FinMag: Finite-Element Micromagnetic Simulation Tool" (2018).
- ⁹⁶F. S. Ma, H. S. Lim, Z. K. Wang, S. N. Piramanayagam, S. C. Ng, and M. H. Kuok, *Appl. Phys. Lett.* **98**, 153107 (2011).
- ⁹⁷G. Venkat, M. Franchin, O. Dmytriiev, M. Mruczkiewicz, H. Fangohr, A. Barman, M. Krawczyk, and A. Prabhakar, *IEEE Trans. Magn.* **49**, 524 (2013).
- ⁹⁸J. W. Klos, D. Kumar, M. Krawczyk, and A. Barman, *Sci. Rep.* **3**, 2444 (2013).
- ⁹⁹F. Ma, Y. Zhou, and W. S. Lew, *IEEE Trans. Magn.* **51**, 1500404 (2015).
- ¹⁰⁰W. Eerenstein and J. N. D. Mathur, *Nature* **442**, 759 (2006).
- ¹⁰¹C.-Y. Liang, S. M. Keller, A. E. Sepulveda, A. Bur, W.-Y. Sun, K. Wetzlar, and G. P. Carman, *Nanotechnology* **25**, 435701 (2014).
- ¹⁰²T. Mathurin, S. Giordano, Y. Dusch, N. Tiercelin, P. Pernod, and V. Preobrazhensky, *Phys. Rev. B* **95**, 140405 (2017).
- ¹⁰³N. Challab, A. D. Aboumassound, F. Zighem, D. Faurie, and M. Haboussi, *J. Phys. D: Appl. Phys.* **52**, 355004 (2019).
- ¹⁰⁴COMSOL Multiphysics, version 4.4, COMSOL AB, Stockholm, Sweden; see www.comsol.com.
- ¹⁰⁵S. Tacchi, F. Montoncello, M. Madami, G. Gubbiotti, G. Carlotti, L. Giovannini, R. Zivieri, F. Nizzoli, S. Jain, A. O. Adeyeye, and N. Singh, *Phys. Rev. Lett.* **107**, 127204 (2011).
- ¹⁰⁶J. W. Klos, M. L. Sokolovskyy, S. Mamica, and M. Krawczyk, *J. Appl. Phys.* **111**, 123910 (2012).
- ¹⁰⁷T. Schwarze, R. Huber, G. Duerr, and D. Grundler, *Phys. Rev. B* **85**, 134448 (2012).
- ¹⁰⁸N. Challab, D. Faurie, M. Haboussi, A. O. Adeyeye, and F. Zighem, *ACS Appl. Mater. Interfaces* **13**, 29906–29915 (2021).
- ¹⁰⁹G. Gubbiotti, A. Sadovnikov, E. Beginin, S. Sheshukova, S. Nikitov, G. Talmelli, I. Asselberghs, I. P. Radu, C. Adelman, and F. Ciubotaru, *Appl. Phys. Lett.* **118**, 162405 (2021).
- ¹¹⁰D. Sheka, *Appl. Phys. Lett.* **118**, 230502 (2021).
- ¹¹¹Y. Gaididei, V. P. Kravchuk, F. G. Mertens, O. V. Pylypovskiy, A. Saxena, D. D. Sheka, and O. M. Volkov, *Low Temp. Phys.* **44**, 634–643 (2018).
- ¹¹²A. Korniienko, V. Kravchuk, O. Pylypovskiy, D. Sheka, J. van den Brink, and Y. Gaididei, *SciPost Phys.* **7**, 35 (2019).
- ¹¹³O. V. Dobrovolskiy, N. R. Vovk, A. V. Bondarenko, S. A. Bunyaev, S. Lamb-Camarena, N. Zenbaa, R. Sachser, S. Barth, K. Y. Guslienko, A. V. Chumak, M. Huth, and G. N. Kakazei, *Appl. Phys. Lett.* **118**, 132405 (2021).